

Land-cover classification based on AVHRR and Geo-spatial data analysis

(Liu Jiuyan, Luo Di, Zhuang Dafang)

Institute of Remote Sensing Applications, C.A.S. Beijing, 100101, China

Abstract

Information regarding the characteristics and spatial distribution of Earth's land cover is critical to global environment research. AVHRR data have been increasingly used in land-cover characterization for large area. Although there have been great progresses in improving the result of classification with geographical knowledge, how to make the best of geo-spatial data remains an open question. As the distribution of land-cover types is the combination of many geo-factors such as terrain, soil, climate and wind, the comprehensive influence of these factors should be taken into account when employing ancillary geo-spatial data for better result of characterization. In this study, effort was made to develop an innovative strategy for land-cover classification of China. By using geo-spatial data such as elevation, precipitation and temperature, a geo-environment image was generated as a band to composite with remotely sensed data for supervised classification. A sample area—Northeast China was used to test the feasibility of this method.

Keywords: NOAA-AVHRR, geo-spatial data, Geo-environment image, Supervised classification

1. Introduction and objectives:

With the growing concern about global change, regional to global land-cover mapping has become an increasingly important data source in a variety of studies such as land-use change, biogeochemical cycle modeling, and climate modeling.

Compared with TM, SPOT imagery, National Oceanic and Atmospheric Administration (NOAA) Advanced Very High Resolution Radiometer (AVHRR) imagery has become a popular alternative for land mapping for large area, because it is relatively inexpensive, has high temporal frequency for avoiding cloud cover, and has moderate data volume for collecting, storing and processing. As AVHRR "Greenness data" such as NDVI are useful for depicting change in vegetative activity over time, we can perform land-cover classification and characterization with AVHRR data based on associations between land-cover types and variations in periodic observance of greenness.

Although during the last decade, substantial progress has been made in using AVHRR data for land-cover characterizations, the result of classification is yet to be further improved. The low accuracy on one hand is due to the coarse spatial resolution and constrained spectral resolution; on the other hand it is also because some disparate land-cover types share spectral reflectance characteristics on the image. When we performing land-cover classification, problems exist in discriminating between land-cover types exhibiting similar phenologies. Such land-cover types often have similar spectral signature on the image, which make it difficult for computer to discriminate different types only based on colorimetry, luminance and the statistic information recorded on the image.

Remote sensing specialists have long recognized the importance of geo-spatial data for land-cover characterization. Significant advances have been made in developing techniques and strategies for using geo-spatial data as ancillary information to improve the result of the land-cover classification. Pettinger (1982) used agricultural, upland, lowland environmental strata and decision rules based on field research to adjust a landsat MSS land-cover classification in Idaho. He showed that the stratification improved both the detail and the accuracy of the map. Cbula and Nyquist (1987) used terrain data and climatological data

(precipitation and climate regimes) in a Landsat Mss classification of Olympic National Park , Washington , resulting in an increased land-cover classes from 9 to 21 as well as an overall accuracy of 91.7 percent.

As geographic information system (GIS) technology has developed , and integrated GIS-Image analysis software has become more common , opportunities for using geo-spatial data and remotely sensed data in concert have expanded. Innovations in data analysis based on expert systems and related techniques facilitate implementation of complex multi-source data analysis strategies. Jesslyn .F. (1994), with the support of remote sensing and GIS, performed land cover classification for the conterminous U.S.. Then she used ancillary data including digital elevation , temperature , precipitation and frost-free-period in post-classification refinement , and got good result.

Although progresses have been made in employing geographic knowledge for land-cover characterization , how to make the best of geo-spatial data remains an open question. What should be kept in mind is that the distribution of land-cover types , especially vegetation types , is limited not by a single factor , but the combination of many environmental factors. How to choose the most influential geo-spatial data and then to exhibit their comprehensive influence on land-cover distribution is important for the further improvement of land-cover characterization.

In this research , an innovative strategy is developed for land-cover characterization for People' s Republic of China , geo-spatial data , including temperature, precipitation and elevation was used as a band to corporate with remote sensing data. The objective of this paper is to present this technique. An example area , Northeast China , was used to test the feasibility of this approach.

2. Method

Any object on the earth surface is closely connected with its environment. The variance on earth surface , especially the natural and physical characteristics of the earth surface , is the main limitation for the distribution of different land-cover types. In many cases , land-cover types which have similar spectral structure on the image , often exhibit variance in their environment. This is why geo-spatial data are required for better accuracy of classification.

In this research , we try to add some environmental information into the image and thus to improve the discriminability of the image. The environmental information here refers to those geo-spatial data that are well-associated with the distribution of vegetation. As previous studies suggest that terrain , moisture and temperature have great influence on the distribution of vegetation in China , we chose these three factors as ancillary data in our land-cover characterization. On the basis of comprehensive analyzing their contribution to vegetation allocation in different areas , a geographical environmental image is made as a "band" to composite with remote sensing data. The image we ultimately for classification is an comprehensive image containing both spectral and geographical environment information.

2.1 Processing flow

The strategy developed to characterize land-cover types employed both geo-spatial and AVHRR data is in a structured manner (Figure 1.)

2.2 Regionalization

Land-cover mapping for large area has unique analysis problem: Continental area typically exhibit greater variation in climate, terrain, vegetation, soil than they are encountered in analysis of small area. Such problem can be dealt with in two ways: first, the study area could be treated as a single one, This

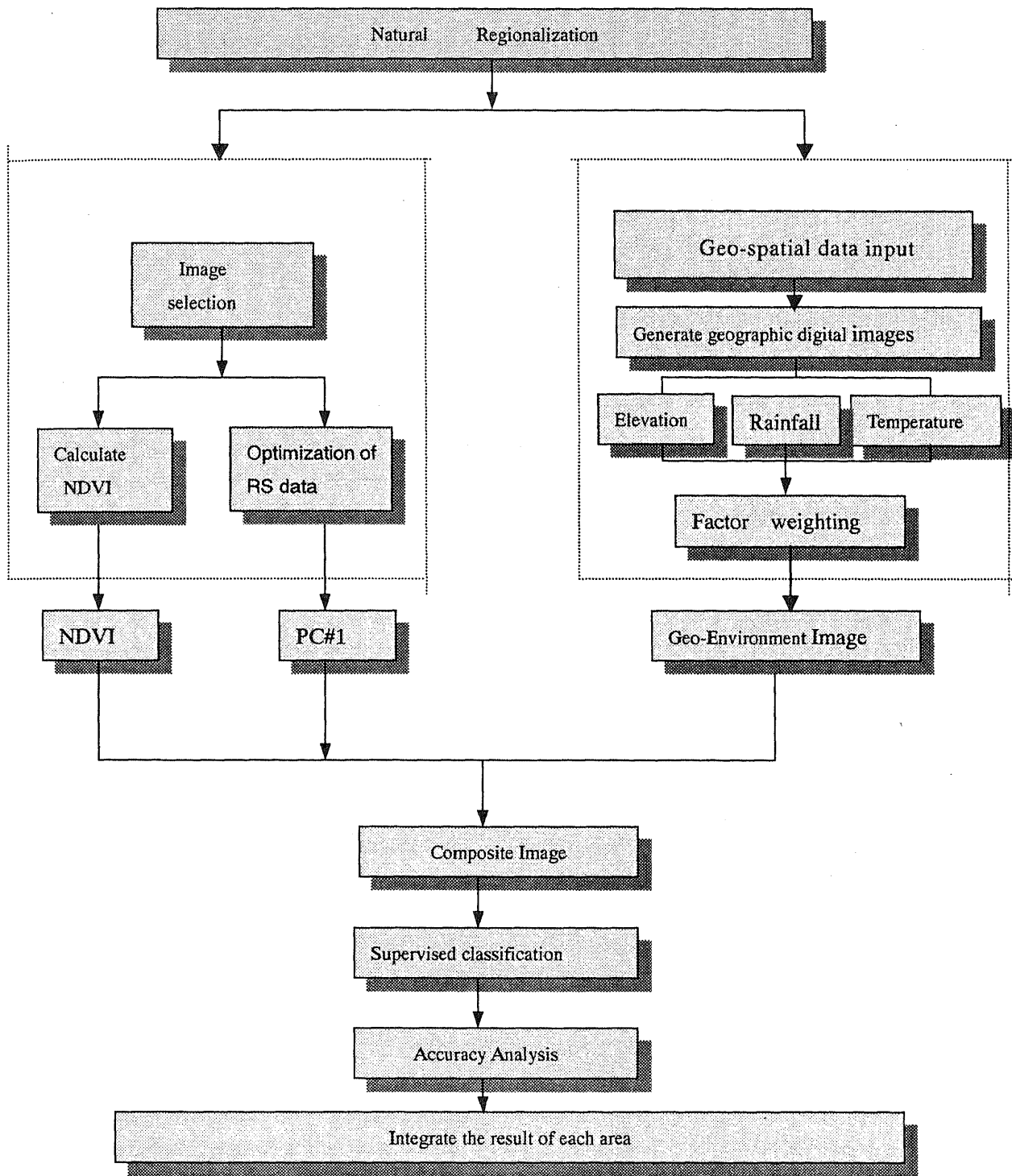


Figure 1. Processing Flow

would serve to avoid the post-classification mosaicing and interregional class correlation problems, but can not limit the environmental diversity. An alternative solution is to partition the area into smaller regions. Given the great environmental variance of China, the latter approach was used in this research.

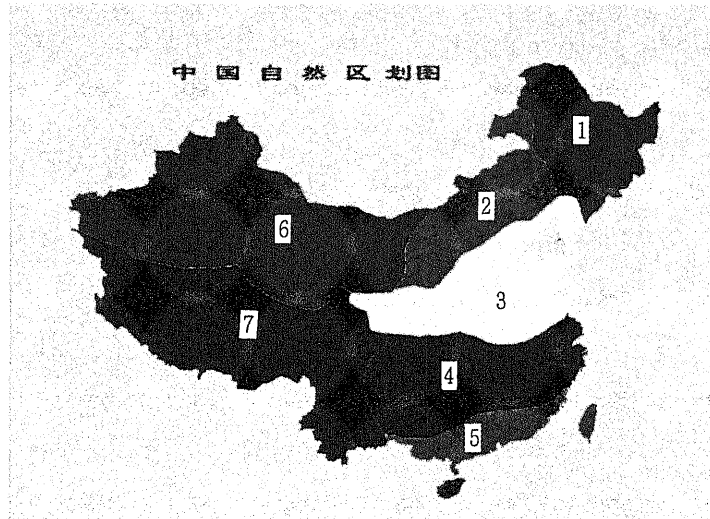


Fig.2 Natural zonation of China

1. Northeast Area
2. InnerMongolia Area
3. Huabei Area
4. Huazhong Area
5. South Area
6. Northwest Area
7. Southwest Area

Facing to the pacific ocean, China is located in the east of Europe-Asia continent and has world' s largest plateau——Tibet Plateau in its southwest Part. The difference of heating power between ocean and land leads to the unique mansion climate which contributes to the regular change in soil、 vegetation within the country. it covers tropical zone、 subtropical zone、 warm temperate zone and temperate zone from south to north and humid plain plateau, semi-arid hilly land and arid desert from east to west. Vegetation distribution seems more complicated. To limit these great diversities, the fist step of our work is to divide China into seven sub-area according to climate、 soil、 terrain and vegetation characteristics in China. There are two advantages by doing so: 1, it contributes to suitable AVHRR image selection according to the phenology of different area; 2, it serves to better analysis of geo-spatial data and thus make a comprehensive "geo-environment" band well reflecting the actual environment of each area.

2.3 Remote sensing image processing and optimization

2.3.1 Selection of suitable images

Phenology is indispensable for image interpretation because it can help to select an image on which disparate vegetation types could be relatively easy to discriminate. There is great phenological variance in China due to its different climate zones; thus it is necessary to select suitable temporal image before classification. As single-data image is often inadequate for land-cover type characterization, multi-date composite images are required.

2.3.2 Calculating NDVI

Vegetation indices are commonly calculated to depicting the growth, coverage and biomass of vegetation on earth surface. Many vegetation indices have been developed for remotely Vegetation monitoring, one of which is Normalized Difference Vegetation Index (NDVI) Derived from the reflectance values of NIR and Visible band, NDVI widely used in studies on soil moisture, crop growth monitoring and vegetation classification.

It is the deference of near-infrared (NIR) and visible (VIS) reflectance values normalized over the sum of those values, as for AVHRR, simply:

$$NDVI = \frac{ch_2 - ch_1}{ch_2 + ch_1}$$

Where ch_2 is the near-infrared band and ch_1 is the visible band.

As a useful vegetation dynamic indicator, NDVI reflects plants' intrinsic biophysichemical characteristic such as biomass, coverage and content of chlorophyll. The definition of NDVI as a ratio helps to suppress the differential solar illumination effect due to surface topography and aspect, and simultaneously emphasize the useful vegetation information. Many researches have showed that NVDI can well capture the dynamic change of vegetation. Goward et al. (1985) used NDVI images from April through November 1982 to map regions of net primary productivity. They show that seasonal NDVI patterns could be associated with major land-cover regions, and that multi-date greenness images could be used to observe patterns of vegetation growth and senescence. In later work, he compared the vegetation characteristics of North and South American biomes by analyzing GVI data using methods developed in Goward's 1985 research. They found that the differential timing and longer duration of the South American growing season was well captured. Biome distributions appeared, qualitatively, well associated with published maps.

In this research, NDVI is calculated for multi-temporal images of each sub-area to represent temporal activities of Vegetation.

2.3.3 Optimization of NOAA-AVHRR data

NOAA-AVHRR has five bands from red to thermal bands. To improve visual effect, we often use colored or false colored image in data processing: choose three bands or channels from multi-band data as red, green and blue channel after data processing. In this study, we intended to integrate temperature, precipitation and elevation data as one band, NDVI MVC image as the second band. Therefore, we could only employ one band from NOAA-AVHRR for false-colored image processing. Because principal components analysis (PCA) can be used to simplify data processing and compress satellite multi-spectral imagery (Richard, 1986), and one of the most important results of PCA is its ability to change pixel definition from M channel sets of number (counts) to K-principal-component (PC) sets ($K < M$) without remarkable loss of (relative) information, we use principal components analysis (PCA) to compress multi-spectral NOAA-AVHRR data.

At the image analysis system, principal component analysis of NOAA-AVHRR data acquired during June 1995 in test site was performed after digitally co-registering and merging. eigenvalues and eigenvectors were subsequently computed. For convenience, comparison of the information content in each principal component (PC) have been titled in ascending order (table1).

A close look at table1 reveals that the first principal component (PC#1) account for 84.8 percent of the total scene variance. In other word, PC#1 contained 84.8 percent information of NOAA-AVHRR data.

Table1. Eigenvalues and eigenvectors of Principal Component Analysis

		PC#1	PC#2	PC#3	PC#4	PC#5
bands	1	0.448	-0.472	0.498	-0.186	0.543
	2	0.369	-0.223	0.246	0.728	0.473
	3	0.320	0.260	-0.508	0.473	0.590
	4	0.727	0.091	0.345	-0.460	-0.363
	5	0.170	0.808	0.561	-0.090	0.037
Eigenvalues		2880.2	297.2	151.3	62.4	32.j
Information capacity		84.8%	.8%	3.7%	1.8%	0.9%
Information accumulation		84.8%	93.6%	97.3%	99.1%	100%

Table2. Correlation matrix from five bands of NOAA--AVHRR

	1	2	3	4	5
1	1.00				
2	0.73	1.00			
3	0.42	0.75	1.00		
4	0.71	0.89	0.82	1.00	
5	0.75	0.90	0.81	0.95	1.00

Therefore, PC#1 has represented the main information of the five bands of NOAA-AVHRR and the humidity and thermal distribution of the ground. It can be used as a representative band for vegetation interpretation and we can use it to co-register with digital image of geographic data and NDVI data.

2. 4 geo-spatial data processing and geo-environment image generation

2.4.1 Generating geographic digital image from geo-spatial data

Average monthly precipitation and monthly mean temperature have been collected from meteorological stations all over the country. At the same time, elevation data were digitized from topology map at a scale of 1 to 1 million. The processing of digital image with geo-spatial data is performed in ARC/INFO system. For each geo-spatial data, we acquired isogram from separated pointed value with grid cell of 1 km, which is suitable for co-registering with AVHRR image; then, process the isogram by interpolation and digital quantifying. After transfer the vector data to raster image, we can get three geographical digital images for terrain($E(x,y)$), precipitation($R(x,y)$) and temperature($T(x,y)$), as presented in figure 3,4,5 respectively.

2.4.2 digital geo-spatial data Weighting and geo-environment image generation

The geo-spatial data mentioned above are used to generate a "geo-environment" image to composite as a band with NDVI and PC#1 data. To get this image, method of weighted-summing was utilized. More specifics, after giving weights to geo-spatial data by analyzing their influence on vegetation distribution, each image will be added together by their weights.

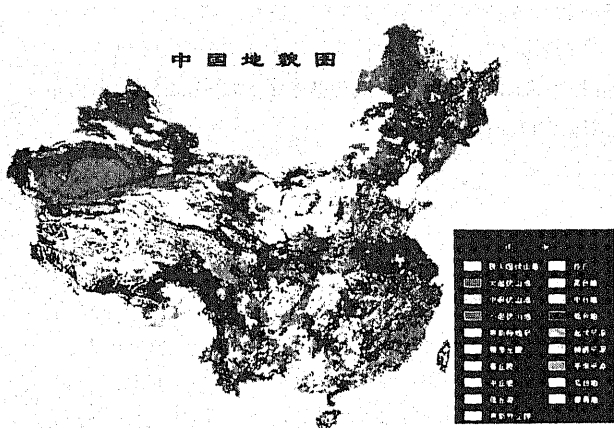


Fig. 3 Geomorphology of China

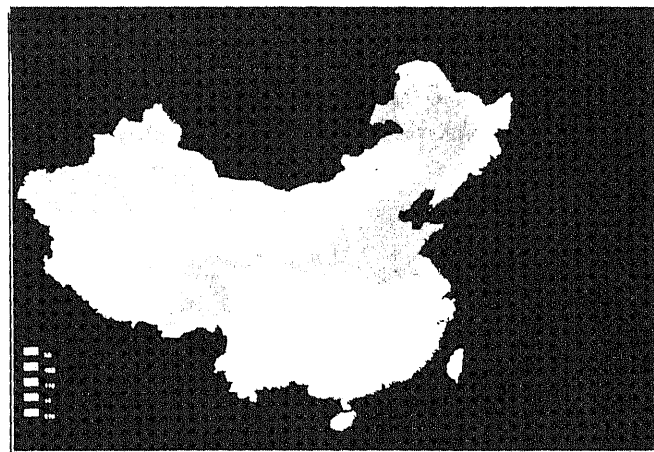


Fig.4 Moisture zone of China

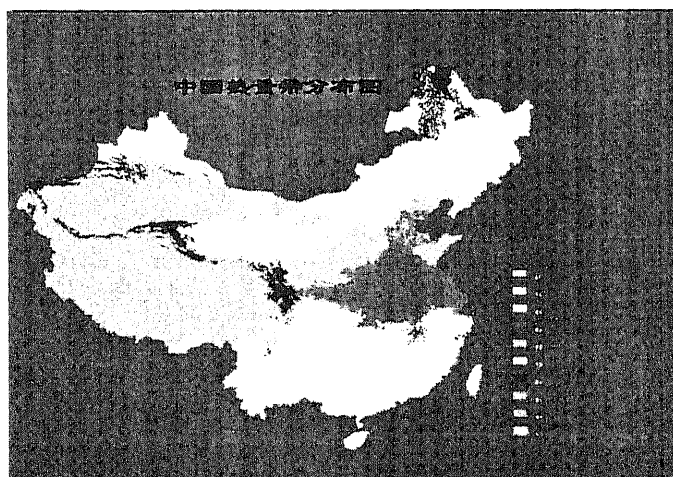


Fig.5 Temperature zone of China

As we know, the distribution of Vegetation results from the combination of many factors, the comprehensive influence of these factors should be given full consideration in analysis of geo-spatial data. Factor weighting is regarded as a crucial step in this research. Although temperature, precipitation and elevation constrict the distribution of vegetation, their contributions to the constriction are not the same. The purpose of weighting is to exhibit the different influence of each factor (In this study, the more the factor has the influence on land-cover distribution, the higher weight it will have). Reasonably weighting means better reflection the actual geographical background by the and thus leads to better result of classification.

Because of the environmental diversity in China, weighting must be based on the particularity of different areas. Driving factor (the geo-spectral -factor which has the highest weigh) can vary by areas. For example, in InnerMongolia Area, the vegetation distribution is constrained dominantly by rainfall, and we can give a high weight to Precipitation to emphasis its importance in this area; while in south China area which has plenty rainfall, precipitation is not the limitation of plant growth. In other words, it should have a relatively low weight.

There are many mathematical processes such as Analytical Hierarchy Process (AHP) and Sequence Synthetically Process for factor weighting in regional resources evaluation. In this study, we employed

AHP for factor weighting of temperature, precipitation and elevation. AHP is an effective process for quantitatively analyzing un-quantitative factors. In AHP, we firstly compute the maximum eigenvalue and its corresponding eigenvector from assessing matrix of evaluating factors and then get the weights for each factor by means of normalizing the maximum eigenvector. The following list the preliminary procedure of AHP:

1). To construct assessing matrix

Given the assessing objective is A and assessing factors are $F = \{f_1, f_2, \dots, f_n\}$,

Then the assessing matrix P can be set as:

$$P = \begin{bmatrix} f_{11} & f_{12} & \dots & f_{1n} \\ f_{21} & f_{22} & \dots & f_{2n} \\ \vdots & \vdots & \vdots & \vdots \\ f_{n1} & f_{n2} & \dots & f_{nn} \end{bmatrix}$$

Where f_{ij} is the value that accounts for the relative importance of f_i compared with f_j , the meaning of the value listed in table 3.

Table 3. The value of f_{ij} and its meaning:

value of f_{ij}	meaning
j	f_i and f_j possessed the same importance for objective A.
3	f_i is a little more important than f_j for objective A.
5	f_i is obviously more important than f_j for objective A
7	f_i is much more important than f_j for objective A
9	f_i is extremely more important than f_j for objective A
2, 4, 6, 8	the mean value between 1 and 3, 3 and 5, 5 and 7, 7 and 9 respectively.
$f_{ji} = 1/f_{ij}$	

2.5 Classification

For accurate integration of remote sensing image and geo-spatial data, the strict registration of multi-source data of different measurement scales is important. In this experiment, a projection transformation is applied to the composite geo-spatial data and remotely sensed data, and we use the same Longitude and Latitude reference frame for registration. Then use the registered geo-environment band with NDVI image and the first Principal Component of AVHRR data to produce the composite image (figure 6).

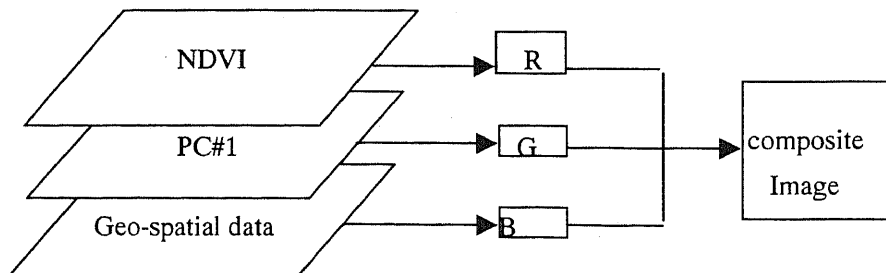


figure 6. Remote sensing and geo-spatial data integration

The composite image, containing both the spectral and the geographic information, is an integrated reflection of physical entity. As we used supervised clustering algorithm and maximum likelihood classification to characterize the land-cover types. Ground samples and published maps in test area have been referred to select training spot in the image.

3. Case study- land-cover classification of Northeastern China

3.1 Description of study area

Northeastern China, the typical vegetation types of which are larch, broad-leaf forest and meadow, covers Arctic-temperate, Temperate-moist and Semi-moist area. According to bio-regions, this region can be divided into three sub-areas : Dawuli, Changbai and Mongolia, corresponding to such land-cover types as conifer, conifer-broadleaf mixed forest and prairie respectively. In this area, winter is cold and long lasting in Northeastern China while summer is temperate but rather short. The average frost-free period is about 100-150 days. Of the whole year, there are 180~190 days (from early April to October) with the mean daily temperature (MDT) above 5 and 120~170 days on which MDT is above 10. Greater than evaporation in the mountain area while a little lower than evaporation in the plain, the precipitation of this area is moderate and decreases from southeast to northwest, from plain to mountain, with the least rainfall mostly in the winter month January and the most in July or August. About sixty percent of total year precipitation concentrates in June to September. Affected by the Southeast Monsoon, precipitation variations are evident among years with average variational rate of 15~20 percent.

3.2 Data collection

The following data are collected:

1. AVHRR data

High temporal density 1 km NOAA-AVHRR images of June 1995 are used in this experiment. After geometric correction, cloud-free processing, projection transformation, we have the NOAA-AVHRR image of Northeastern China (figure 6).

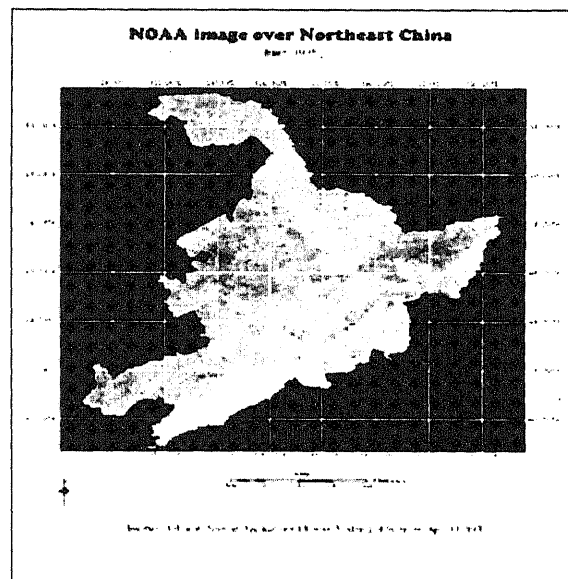


Fig.6 NOAA_AVHRR Image of Northeast China

2. Terrain data

Elevation data recorded by National Observatories.

3. Climate data

Monthly mean precipitation recorded by 361 National Meteorological Observatories.

4. Others

Natural zonation maps, administrative boundary maps, vegetation maps, Land-use maps, etc.

3.3 Remote Sensing data processing

Then process them in ERDAS/IMAGINE to make NDVI images (figure 7) and the first Principal Component image (Fig. 8)

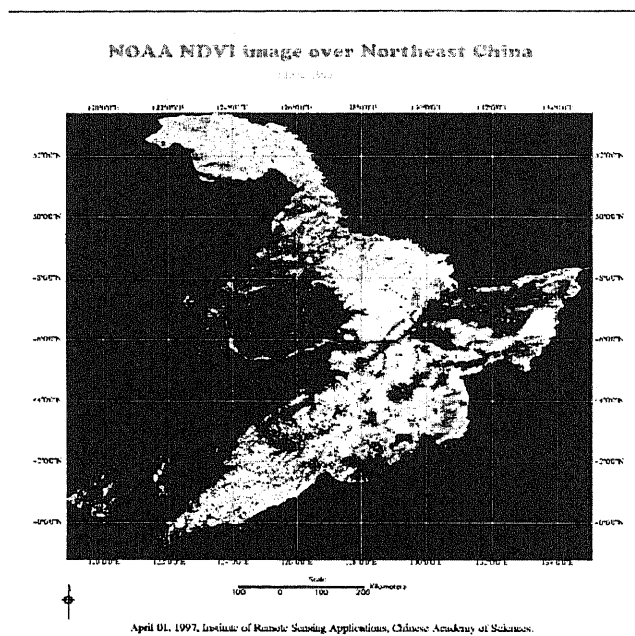


Fig.7 NDVI image over Northeast China

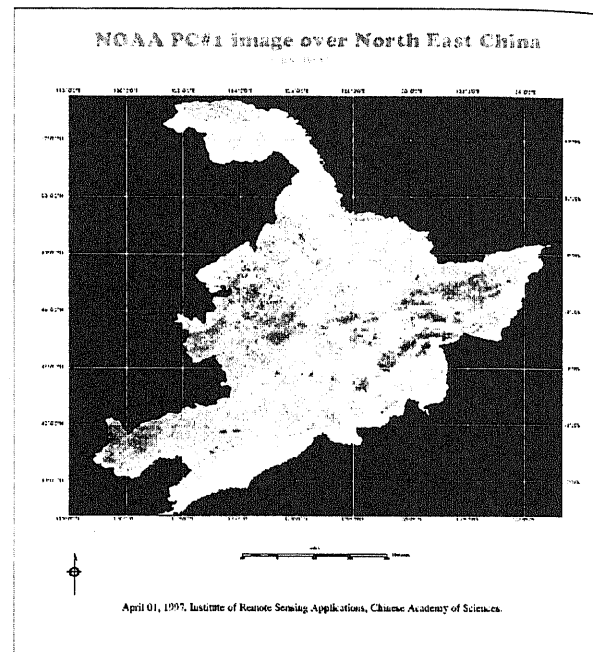


Fig.8 NOAA PC#1 image over Northeast China

3.4 Geo-spatial data processing and weighting

Collect the monthly mean temperature, precipitation and altitude data, and input them into the computer. Transform the point file into isograms, then digitize the isogram using interpolation, and transform the vector map into raster image. The resulting geographical digital images of Northeastern China are mean temperature image of June (figure 9), mean precipitation image of June (figure 10) and elevation image (figure 11).

In study area, when we analyze the relationship between vegetation and temperature, precipitation and elevation, we can learned that: temperature is a driving factor affecting the vegetation growth; precipitation affects the vegetation growth coordinated with temperature; the influence on vegetation growth from elevation is not somewhat less important than that of temperature and precipitation.

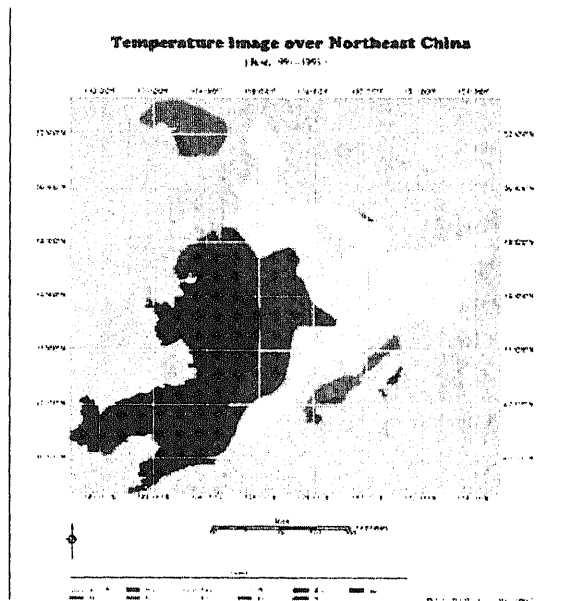


Fig.9 Monthly mean temperature of June

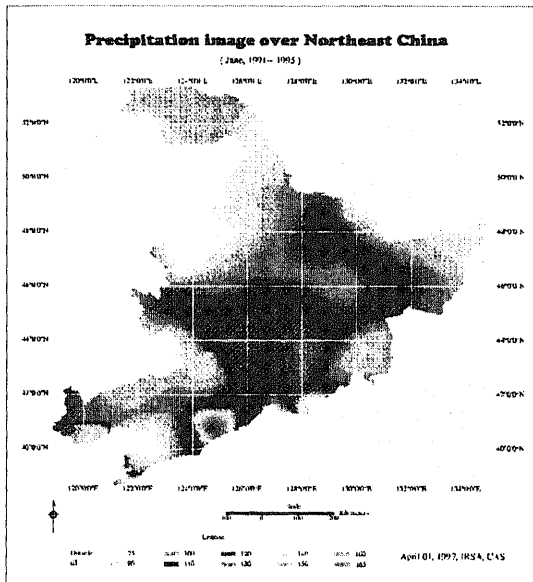


Fig.10 Monthly mean precipitation of June

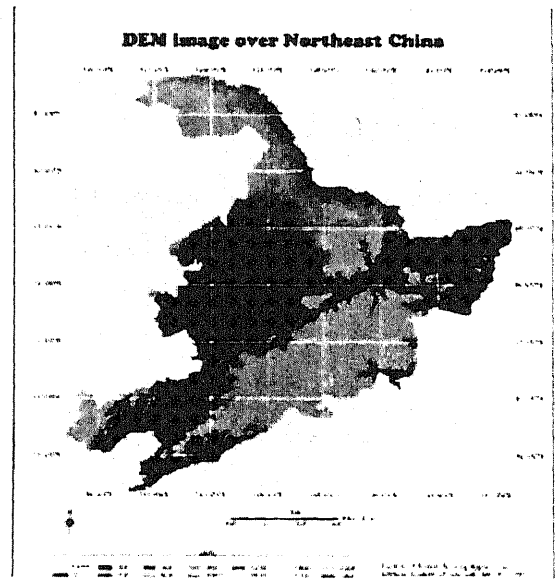


Fig.11 DEM image of Northeast China

Therefore, according to AHP, we can define the assessing matrix as follows:

	F ₁	F ₂	F ₃
F ₁ (temperature)	1	2	3
F ₂ (precipitation)	$\frac{1}{2}$	1	3
F ₃ (elevation)	$\frac{1}{3}$	$\frac{1}{3}$	1

2). Eigenvalue (d) and eigenvector and assessing matrix

$$d = \begin{bmatrix} 3.0536 & 0 & 0 \\ 0 & -0.0268 + 0.4038i & 0 \\ 0 & 0 & -0.0268 - 0.403i \end{bmatrix}$$

$$X = \begin{bmatrix} 0.8257 & 0.5674 + 0.5998i & 0.5674 - 0.5998i \\ 0.5201 & -0.5060 + 0.1206i & -0.5060 - 0.1206i \\ 0.2184 & 0.0624 - 0.2094i & 0.0624 + 0.2094i \end{bmatrix}$$

3).the weight of each factor

by means of normalizing the eigenvector,we can get the weight of each factor:

$$\alpha_1 = \frac{0.8257}{0.8257 + 0.5201 + 0.2184} = 0.527$$

$$\alpha_2 = \frac{0.5201}{0.8257 + 0.5201 + 0.2184} = 0.333$$

$$\alpha_3 = \frac{0.2184}{0.8257 + 0.5201 + 0.2184} = 0.140$$

Now, we can define the integrated geo-environment image as:

$$G(x, y) = 0.527 \times T(x, y) + 0.333 \times P(x, y) + 0.140 \times E(x, y)$$

G (x, y) (Figure 12) then can be used as an independent geographic information “band” to composite with remote sensing data.

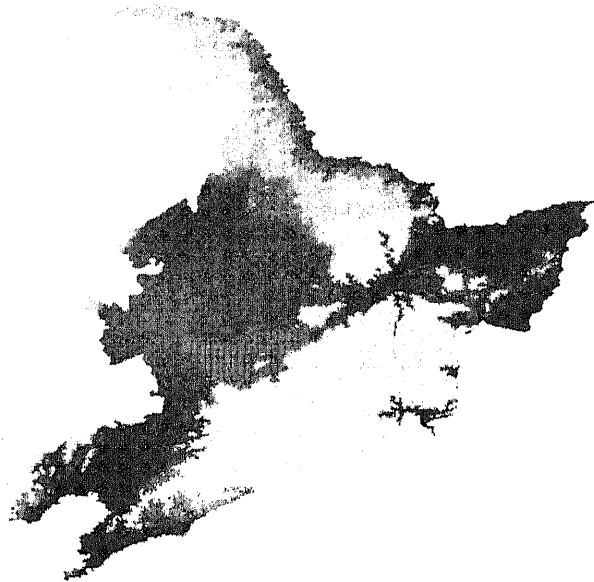
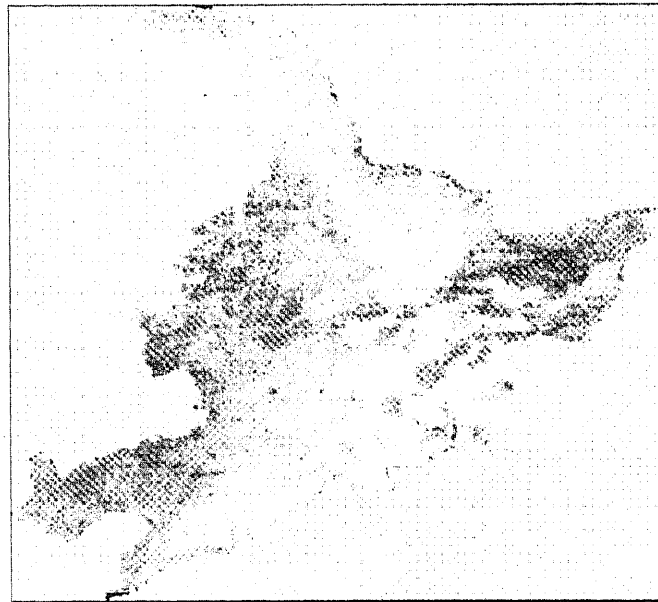


Fig.12 Geo-environment image



**Fig.13 Composite image generated by
Geo-spatial data and remotely sensed data**

3.5 Integration of geo-spatial data with remote sensing image

After the process of projection transformation and registration of the geo-spatial data and the remote sensing image, we use the geo-environment image, the NDVI image and the PC#1 image of NOVAA-AVH RR as three bands and get a composite image (figure 13).

To test the contribution of geo-spatial data to the new composite image, we analyzed the information capacity of this composite image. The results are showed in chart 4, 5 and 6.

The charts showed that, as a result of incorporating geo-spatial data into remotely sensed data, the

dimension of the original NOAA-AVHRR data increases from 4 to 7. Compared the three chart, we can also find that the climate data $T(x, y)$ and the precipitation data $P(x, y)$ are highly correlated with each NOAA-AVHRR spectral band, while this correlation are relatively small in the case of the altitude data $E(x, y)$.

Chart 4. Information capacity analyses of original NOAA-AVHRR data after the addition of altitude data

Band		Correlation matrix						Principle Component	Eigenvalue	Percent of information capacity	Accumulated Percent of Information Capacity
N O A A	1	1.00	0.73	0.42	0.71	0.75	0.14	1	2533	75.3%	75.3%
	2		1.00	0.75	0.89	0.90	0.60	2	.8	13.1%	88.4%
	3			1.00	0.82	0.81	0.40	3	441.	6.7%	95.1%
	4				1.00	0.95	0.39	4	6	2.7%	97.8%
	5					1.00	0.35	5	244.	1.4%	99.2%
$E(x, y)$							1.00	6	0	0.8%	100%
								7	91.2		
								8	48.6		
								9	26.7		

Chart 5. Information capacity analyses of NOAA-AVHRR data after the addition of altitude and temperature

Band		Correlation Matrix							Principle Component	Eigenvalue	Percentage of information capacity	Accumulated Percent of Information Capacity
N O A A	1	1.00	0.73	0.42	0.71	0.75	0.14	0.77	1	2213.8	71.7%	71.7%
	2		1.00	0.75	0.89	0.90	0.60	0.91	2	456.4	14.8%	86.5%
	3			1.00	0.82	0.81	0.40	0.78	3	229.2	7.4%	93.9%
	4				1.00	0.95	0.39	0.82	4	92.1	3.0%	96.9%
	5					1.00	0.35	0.75	5	49.4	1.6%	98.5%
$E(x, y)$							1.00	0.46	6	36.5	1.2%	99.7%
$T(x, y)$								1.00	7	8.6	0.3%	100%

Chart 6. Information capacity analyses of NOAA-AVHRR data corporated with altitude, temperature and precipitation data

波段		Correlation Matrix							Principle Component	Eigenvalue	Percentage of information capacity	Accumulated Percent of Information Capacity	
N O A A	1	1.0	0.73	0.42	0.71	0.75	0.14	0.77	0.73	1	2244.6	67.2%	67.2%
			1.0	0.75	0.89	0.90	0.60	0.91	0.87	2	422.8	12.7%	79.9%
				1.0	0.82	0.81	0.40	0.78	0.72	3	268.0	8.0%	87.9%
					1.0	0.95	0.39	0.82	0.84	4	186.4	5.6%	93.5%
						1.0	0.35	0.75	0.87	5	98.6	3.0%	96.5%
$E(x, y)$							1.0	0.46	0.38	6	68.8	2.1%	98.6%
$T(x, y)$								1.0	0.69	7	36	1.0%	99.6%
$P(x, y)$								1.0		8	16	0.4%	100.0%

3.6 Supervised classification

Given the similar spectral character between meadow and some forest, we adopt the method of Binary Tree to divide the composite image into forest and non-forest, then performed supervised classification respectively (Figure 14, Figure 15). In practice, we get forest distribution map of Northeastern from “Resources and Environment Database of China ” by GIS to perform the division

From the classification result, the integrated image can be classified as broadleaf forest, mixed needleleaf and broadleaf forest, needleleaf forest, shrub, miscellaneous forest, poplar and birch, farmland, meadow, marsh, grassland, reed marshes and lake twelve kinds of land-cover types (fig.16). Classification accuracy is 78.72% for forest and 78.9% for non-forest. The overall accuracy is 78.81%.

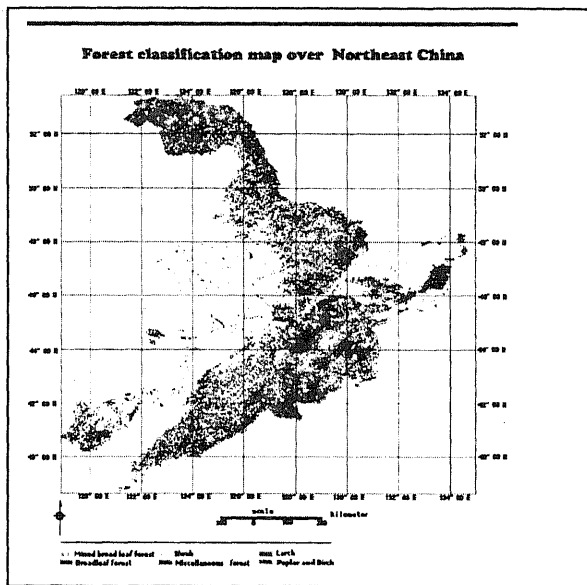


Fig.14 Non-forest classification map

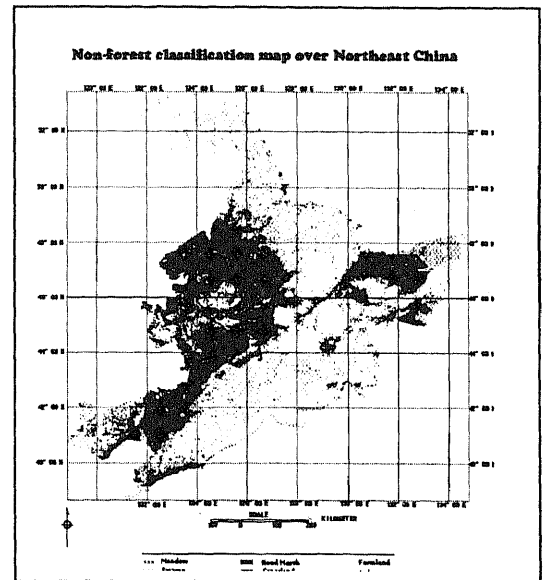


Fig.15 Forest classification map

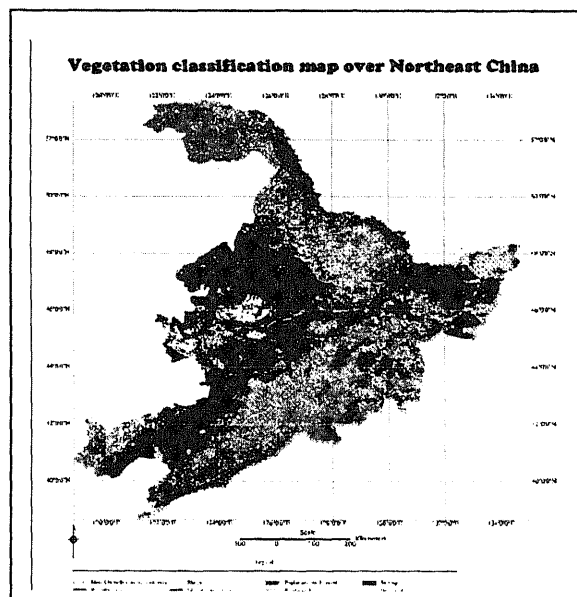


Fig.16 Land-cover classification of Northeast China

4. Conclusion

- 1). The spectral information structure of remote sensing data can be improved by means of integrating digital geographic data with remote sensing. The integrated image reflected not only the present condition of vegetation but also its internal causes(geographic factors).
- 2). The methodology of using multi-temporal remote sensing images, coupled with digital geographic image integrated in GIS for vegetation classification proved to be feasible and better than the conventional digital classification method alone. This approach is effective for discriminating land-cover types which have similarity on spectral structure but have relatively more difference in their environment.
- 3). Although remote sensing and GIS are two relatively independent techniques, they are related to each other because of the same study objective. By means of integrating different data in GIS environment, not only the accuracy of remote sensing information interpretation can be improved, but remote sensing can used as a data resource for GIS system analysis. In this sense, this two techniques are mutual assisted.

References

- Zhu qijing, 1991. A Study on Vegetation Classification Using Multi-Temporal NOAA-AVHRR Data: *environment and remote sensing*, vol. 6. No. 2
- Wu Bingfang, Huang Xun, Tian Zhigang, 1995. Vegetation Classification Using Remote Sensing And GIS: *environment and remote sensing*, vol. 10, no.1
- Gervin, J. C., A. G. Witt, Y. C. Lu, And R. Sekhon, 1989. Comparison of Level 1 Land Cover Classification Accuracy for MSS and AVHRR Data: *International Journal of Remote Sensing*, Vol. 6, No. 1, Pp.47-57
- Goward, S. N., D. G. Dye, 1985. North American Vegetation Patterns Observed with the NOAA-7 Advanced Very High Resolution Radiometer: *Vegetatio*, Vol.64, Pp. 3-14
- Holben, B., 1988, Characteristics Of Maximum Value Composite Images from Temporal AVHRR Data, *International Journal Of Remote Sensing*, Vol. 7, Pp.1417-1434
- James M.E, and Kalluri S.N., 1994, The Pathfinder AVHRR Land Data Set: An Improved Coarse Resolution Data Set for Terrestrial Monitoring. , *International Journal of Remote Sensing Vol.15, No.17*.
- Jesslyn F. Brown, Thomas R. Loveland, James W. Merchant, Bradley C. Reed, Donald O. Ohlen, 1993. Using Multisource Data in Global Land-Cover Characterization: Concepts, Requirements, And Methods: *Photogrammetric Engineering & Remote Sensing*, Vol. 59, No. 6 Pp.977-987
- Justice, C. O., J. R. G. Townshend, B. N. Holben, And C. J. Tucker, 1985 Analysis Of Phenology Of Global Vegetation Using Meteorological Satellite Data: *International Journal of Remote Sensing*, Vol. 6, Pp. 1271-1318
- Lloyd, D., 1991, A Phenological Classification of Terrestrial Vegetation Using Shortwave Vegetation Index Imagery: *International Journal of Remote Sensing*, Vol. 11, No. 12, and Pp.2269-2279
- Thomas R. Loveland, James W. Merchant, Donald O. Ohlen And Jesslyn F. Brown, 1991. Development of A Land-Cover Characteristics Database for the Conterminous U. S.: *Photogrammetric Engineering & Remote Sensing*, Vol. 57, No. 11, Pp.1453-1463
- Townshend, J. R. G., And C. J. Tucker, 1984, Objective Assessment of Advanced Very High Resolution Radiometer Data for Land Cover Mapping: *International Journal of Remote Sensing*, Vol.5, No. 2, and Pp.497-504
- Townshend, J. R. G., And C. O. Justice, 1988, selecting The Spatial Resolution for Satellite Sensor Required For Global Monitoring of Land Transformations: *International Journal of Remote Sensing*, Vol. 8, No. 2, Pp. 187-236
- Townshend, J. R. G., C. O. Justice, And V. Kalb, 1987, Characterization and Classification of South American Land Cover Types: *International Journal of Remote Sensing*, Vol. 8, No.8, and Pp.1189-1207
- Tucker, C. J., J. A. Gatin, And S. R. Schneider, 1984. Monitoring Vegetation in The Nile Delta with NOAA-6 AND NOAA-7 AVHRR Imagery: *Photogrammetric Engineering & Remote Sensing*, Vol. 50, No. 1, Pp. 53-61